Tracking Trajectory of Underactuated Surface Vessels: a Numerical Method Approach

Mario E. Serrano*, Gustavo J. E. Scaglia*, Vicente Mut*, Oscar A. Ortiz*, Mario Jordan**

**National University of San Juan, Argentine*
phone: +549 264 4211700, fax: +54 264 4227216;
e-mail: serranoemanuel84@gmail.com, gscaglia@unsj.edu.ar, vmut@unsj.edu.ar, rortiz@unsj.edu.ar).
***Argentine Institute of Oceanography*
e-mail: mjordan@criba.edu.ar.

Abstract: The main difficulty in the control of an underactuated system is that the system has more outputs to be controlled than the number of independent inputs. In this paper a novel trajectory tracking controller designed originally for robotic systems is applied for underactuated surface ships. A simple approach is proposed to track trajectories, knowing the desired state, a value for the control action needed to force the system to go from its current state to a desired one can be obtained. Its main advantage is that the condition for the tracking error tends to zero and the calculation of control actions, are obtained solving a system of linear equations. In addition, the convergence to zero of tracking errors and simulation results are included in this article.

Keywords: Control System Design, Linear Algebra, Nonlinear Model, Tracking Trajectory Control.

1. INTRODUCTION

Stabilisations and tracking control of position (sway and surge) and orientation (yaw) of underactuated surface ships have recently received considerable attention from the control community, see for example, (Lefeber et al., 2003; Ghommam et al., 2006; Wondergem et al., 2011), and many others. The challenge of these problems is due to the fact that the motion of the underactuated ship in question possesses three degrees of freedom (yaw, sway and surge neglecting the motion in roll, pitch and heave) whereas there are only two available controls (surge force and yaw moment). The use of trajectory tracking for a vessel system is justified in structured workspaces as well as in partially structured workspaces, where unexpected obstacles can be found during the navigation. In the first case, the reference trajectory can be set from a global trajectory planner. In the second case, the algorithms used to avoid obstacles usually re-plan the trajectory in order to avoid a collision, generating a new reference trajectory from this point onwards. Usually, the goal is to find the combined control actions to track the reference trajectory, defined by the variables x_{ref} and y_{ref}.

In (Lefeber et al., 2003), researchers address the tracking problem for an underactuated ship using two controls, namely surge force and yaw moment. A state-feedback control law is developed and proved to render the tracking error dynamics globally k–exponentially stable. However, it requires a change of coordinates to find the control law. In (Wondergem et al., 2011), an observer-controller scheme to track a trajectory in real-time using the position and heading measurements of the ship is proposed. In the observer design the dynamic ship model in the Earth fixed frame is considered, which has the advantage that the properties of the Coriolis and centripetal matrix written in Christoffel symbols can be used. In the controller design the dynamic ship model in the bodyfixed frame is considered, so that the stabilizing terms can be chosen with respect to the forward, sideward and orientation error. Disregarding the rotations, the closed-loop system can be tuned like a second-order system.

(Ghommam et al., 2006), considers the problem of controlling the planar position and orientation of an autonomous surface vessel using two independent side thrusters. Two transformations are introduced to represent the system into a pure cascade form. They show through some key properties of the model that the global and uniform asymptotic stabilization problem of the resulting cascade system can be reduced to the stabilization problem of a third-order chained form. A discontinuous backstepping approach is then employed for the stabilization of the chained form system via a partial state feedback. In (Do et al., 2002a), a single controller, called universal controller, which solved both stabilization and tracking simultaneously is shown. The authors proposed a controller based on Lyapunov's direct method and the backstepping technique. In most existing backstepping-based techniques, a very restrictive assumption is that yaw reference velocity has to satisfy persistent excitation conditions and thus it does not converge to zero. Consequently, a vessel cannot track straight-line reference trajectories, which is unrealistic in practice.

Based on Lyapunov direct method and passivity, (Jiang, 2002), proposed two constructive tracking solutions for the underactuated ship. However, in both (Do et al., 2002b and Jiang, 2002), authors imposed the yaw velocity to be non-zero. In (Ghommam et al., 2009), a feedback controller that forces the ship to exponentially follow the desired trajectory from any initial conditions is shown. Using a cascade approach, they show that the tracking error dynamics of the ship can be decomposed as a cascade of one non-linear system (driven subsystem) and a first-order chained form system with integrator (driving subsystem). Tracking control of ships has mainly been based on linear models, giving local results, and steering only two degrees of freedom. In (Oh and Sun, 2010), an MPC scheme with line of sight was presented for tracking problems of underactuated vessels based on linearization.

In this work a trajectory-tracking controller, designed originally for robotic systems (Scaglia et al., 2008; Scaglia et al., 2009; Scaglia et al., 2010; Rosales et al., 2011), is applied for underactuated surface ships. The originality of this control approach is based on the application of linear algebra for trajectory tracking, where the calculation of control actions, are obtained solving a system of linear equations. This work presents a novel trajectory-tracking controller suitable for embebed applications. Furthermore, the algorithm developed is easier to be implemented in a real system because the use of discrete equations allows direct adaptation to any computer system or programmable device running sequential instructions to a programmable clock speed.

The methodology developed for tracking the trajectory of reference $\{(x_{ref}, y_{ref})\}$ is based on determining the desired trajectories of the remaining state variables. These states are determined by analysing the conditions so that the system of linear equations has exact solution. The main contribution of this work is the application of the control technique based on linear algebra, to design tracking controllers applied to vessel systems. In this paper the methodology is validated through simulation results. In addition, proofs of the zero-convergence of the tracking error are included in this paper.

The paper is organized as follows: Section 2 presents the methodology for the design of a control system, using linear algebra. Section 3 shows the results of simulation, by applying the methodology proposed in the Cybership I example (Bao-li, 2009; Ghommam et al., 2009). Finally, Section 4 presents the conclusions and some topics that will be addressed in future contributions.

2. METHODOLOGY FOR CONTROLLER DESIGN

2.1 Nomenclature and design methodology

Let us consider the first-order differential equation,

$$\frac{dy}{dt} = \dot{y} = f(y,t,u) \qquad y(0) = y_0 \tag{1}$$

In (1) y represents the output to the system to be controlled, u is the control action, and t is the time. The values of $y(t)$ at discrete time $t=nT_0$, where T_0 is the sampling period and $n\in\{0, 1, 2, ...\}$, will be denoted as $y_{(n)}$. Thus, when computing $y_{(n+1)}$ by knowing $y_{(n)}$, (1) should be integrated over the time interval $nT_0 \le t \le (n+1)T_0$ as follows:

$$y_{(n+1)} = y_{(n)} + \int_{nT_0}^{(n+1)T_0} f(y,t,u)dt \tag{2}$$

Where, u remains constant during the interval $nT_0 \le t \le (n+1)T_0$. Therefore, if one knows beforehand the reference trajectory (referred to as $y_{ref}(t)$) to be followed by $y(t)$, then $y_{(n+1)}$ can be substituted by $y_{ref(n+1)}$ into (2), then it is possible to calculate $u_{(n)}$ that represents the control action required to go from the current state to the desired one.

There are several numerical integration methods to calculate the integral in (2). For instance, the Euler method approaches can be used,

$$y_{(n+1)} \cong y_{(n)} + T_0 f(y_{(n)}, t_{(n)}, u_{(n)}) \tag{3}$$

The use of numerical methods in the simulation of the system is based mainly on the possibility to determine the state of the system at instant $n+1$ from the state, the control action, and other variables at instant n. So, $y_{(n+1)}$ can be substituted by a function of reference trajectory and then the control action to make the output system evolve from the current value ($y_{(n)}$) to the desired one can be calculated. To accomplish this, it is necessary to solve a system of linear equations for each sampling period, as shown in next Section. This represents an important advantage mainly for two reasons, first for complex systems (linear or nonlinear), the equations can be solved using iterative methods for solving systems of linear equations, which only need an initial value to start the iteration. This value may be precisely the estimate calculated in the previous sampling instant. Second, this methodology can be applied to other types of systems and the accuracy required by the numerical method is less than the one needed to simulate the behavior of the system under study. This is because, when state variables are available for feedback, at each sampling instant, the method corrects any differences caused by the cumulative error (for example, "rounding errors"). So, the approximation is used to find the best way to go from one state to the next, according to the availability of the system model

2.2 Ship Model

Marine vessels require six independent coordinates to determine their complete configuration (position and orientation) and only two available controls (surge force and yaw moment). The six different motion components are conveniently defined as surge, sway, heave, roll, pitch and yaw (see Fig. 1). Since we seek to control the ship motion in the horizontal plane, it is common to reduce the general six degrees of freedom model to motion in surge, sway and yaw only. This is done by neglecting the heave, roll and pitch modes, which are open-loop stable for most ships (Bao-li, 2009; Ghommam et al., 2009; Lefeber et al., 2003). This nonlinear multivariable model (Fig. 1) ship with only two propellers has been used by others authors (Bao-li, 2009; Ghommam et al., 2009), it is given by,

$$\begin{cases} \dot{x} = u\ \cos(\psi) - v\ \sin(\psi) \\ \dot{y} = u\ \sin(\psi) + v\ \cos(\psi) \\ \dot{\psi} = r \\ \dot{u} = \dfrac{m_{22}}{m_{11}}\ v\ r - \dfrac{d_{11}}{m_{11}} u + \dfrac{1}{m_{11}} T_u \\ \dot{v} = -\dfrac{m_{11}}{m_{22}}\ u\ r - \dfrac{d_{22}}{m_{22}}\ v \\ \dot{r} = \dfrac{m_{11} - m_{22}}{m_{33}}\ v\ u - \dfrac{d_{33}}{m_{33}}\ u + \dfrac{1}{m_{33}} T_r \end{cases} \tag{4}$$

Where $(x,y) \in R^2$ is the position of the ship given in an inertial frame and $\psi \in [0, 2\pi)$ is the heading angle of the ship relative to the geographic North. The general kinematic equations of motion of the vehicle in the horizontal plane can be developed using a global coordinate frame {U} and a body-fixed coordinate frame {B}, as depicted in Fig. 1. Here, u is the forward velocity (surge), v is the transverse velocity (sway) and r is the angular velocity in yaw. The parameters $m_{ii}>0$ are given by the ship inertia and added mass effects. The parameters $d_{ii}>0$ are given by the hydrodynamic damping. The available control inputs are the surge control force T_u and the yaw control moment T_r.

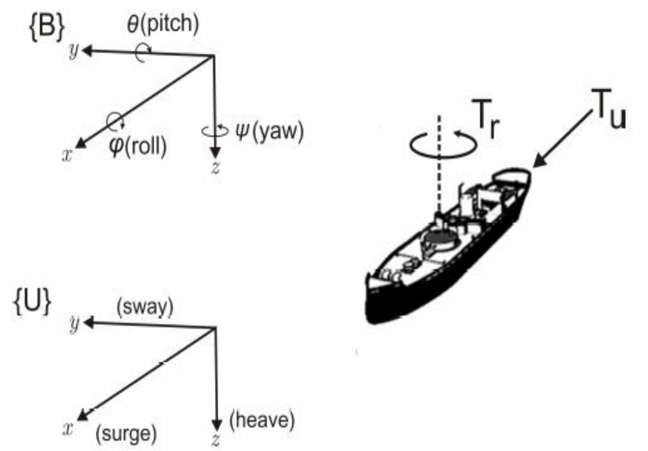

Fig. 1. Marine Vessel: global coordinate frame {U} and a body-fixed coordinate frame {B}.

2.3 Controller Design

The aim of this work is to generate the values of T_u and T_r, so that the Marine vessels can follow a pre-established trajectory. In order to accomplish that, a methodology based on linear algebra and numerical methods is developed.

The first step of the proposed methodology is order the linear first order differential equations writing them in matrix form:

$$\begin{bmatrix} 0 & 0 \\ 0 & 0 \\ 0 & 0 \\ 0 & 0 \\ \dfrac{1}{m_{11}} & 0 \\ 0 & \dfrac{1}{m_{33}} \end{bmatrix} \begin{bmatrix} T_u \\ T_r \end{bmatrix} = \begin{bmatrix} \dot{x} - \left(u\ \cos(\psi) - v\ \sin(\psi)\right) \\ \dot{y} - \left(u\ \sin(\psi) + v\ \cos(\psi)\right) \\ \dot{\psi} - r \\ \dot{v} - \left(-\dfrac{m_{11}}{m_{22}}\ u\ r - \dfrac{d_{22}}{m_{22}}\ v\right) \\ \dot{u} - \left(\dfrac{m_{22}}{m_{11}}\ v\ r - \dfrac{d_{11}}{m_{11}} u\right) \\ \dot{r} - \left(\dfrac{m_{11} - m_{22}}{m_{33}}\ v\ u - \dfrac{d_{33}}{m_{33}}\ u\right) \end{bmatrix} \tag{5}$$

Through the Euler's approximation of the nonlinear model of the marine vessel (5), the following set of equations is obtained:

$$\begin{bmatrix} 0 & 0 \\ 0 & 0 \\ 0 & 0 \\ 0 & 0 \\ \dfrac{1}{m_{11}} & 0 \\ 0 & \dfrac{1}{m_{33}} \end{bmatrix} \begin{bmatrix} T_{u(n)} \\ T_{r(n)} \end{bmatrix} = \begin{bmatrix} \left(\dfrac{x_{(n+1)} - x_{(n)}}{T_0}\right) - \left(u_{(n)} \cos(\psi_{(n)}) - v_{(n)} \sin(\psi_{(n)})\right) \\ \left(\dfrac{y_{n+1} - y_{(n)}}{T_0}\right) - \left(u_{(n)} \sin(\psi_{(n)}) + v_{(n)} \cos(\psi_{(n)})\right) \\ \left(\dfrac{\psi_{(n+1)} - \psi_{(n)}}{T_0}\right) - r_{(n)} \\ \left(\dfrac{v_{(n+1)} - v_{(n)}}{T_0}\right) - \left(-\dfrac{m_{11}}{m_{22}} u_{(n)}\ r_{(n)} - \dfrac{d_{22}}{m_{22}} v_{(n)}\right) \\ \left(\dfrac{u_{(n+1)} - u_{(n)}}{T_0}\right) - \left(\dfrac{m_{22}}{m_{11}} v_{(n)}\ r_{(n)} - \dfrac{d_{11}}{m_{11}} u_{(n)}\right) \\ \left(\dfrac{r_{(n+1)} - r_{(n)}}{T_0}\right) - \left(\dfrac{m_{11} - m_{22}}{m_{33}} v_{(n)}\ u_{(n)} - \dfrac{d_{33}}{m_{33}} r_{(n)}\right) \end{bmatrix} \tag{6}$$

Now we will consider the problem of designing a control law capable of generating the signals $T_{u(n)}$ and $T_{r(n)}$, with the objective that the ship follows the reference trajectory $\{(x_{ref(n+1)}, y_{ref(n+1)})\}$. In order to the problem always have a unique solution is necessary that the system of linear equations (6) have exact solution.

Remark 1: To calculate $T_{u(n)}$ and $T_{r(n)}$, the system of equations (6) must have an exact solution. Thus, the values of the variables (u, ψ, r) are determined to the tracking error tends to zero (see Appendix).

Remark 2: In this work is assumed the fact the state variables are available, by measurement, at any time n, then in (6) $(x_{(n)}, y_{(n)}, \psi_{(n)}, v_{(n)}, u_{(n)}, r_{(n)})$ are the values taken by each variables at n instant.

Remark 3: The value of the difference between the reference and real trajectory will be called tracking error. It is given by $e_{x(n)}=x_{ref(n)}-x_{(n)}$ and $e_{y(n)}=y_{ref(n)}-y_{(n)}$, the tracking error being represented by:

$$\left\|e_{(n)}\right\| = \sqrt{\left(e_{x(n)}^{\;2} + e_{y(n)}^{\;2}\right)}$$

The use of discrete-time model (6) in the simulation of the system is based mainly on the possibility to determine the state of the system at instant *(n+1)* from the state, the control action, and other variables at instant *(n)*. So, in system (6) $\{(x_{(n+1)}, y_{(n+1)})\}$ can be substituted by a function of reference trajectory $\{(x_{ref(n+1)}, y_{ref(n+1)})\}$ and then the control action to make the output system evolve from the current value to the desired one can be calculated. So, the approximation is used to find the best way to go from one state to the next, according to the availability of the system model. Considering it and using discrete-time system, $\{(x_{(n+1)}, y_{(n+1)})\}$ in system (6) can be replaced by a function of reference trajectory $\{(x_{ref(n+1)}, y_{ref(n+1)})\}$. Then, the following equations are defined,

$$x_{(n+1)} = x_{ref(n+1)} - k_x\ \underbrace{(x_{ref(n)} - x_{(n)})}_{e_{x(n)}} \tag{7}$$

$$y_{(n+1)} = y_{ref(n+1)} - k_y\ \underbrace{(y_{ref(n)} - y_{(n)})}_{e_{y(n)}} \tag{8}$$

where k_x *and* k_y are controller's parameters and fulfil $0<k_x<1$ and $0<k_y<1$ to the tracking error tends to zero (see Appendix).

Remark 4: This approach is commonly used in control theory in the design of inverse dynamics controllers and has been used in several recent papers (Scaglia et al., 2008; Scaglia et al., 2009; Rosales et al., 2009; Scaglia et al., 2010; Rosales et al., 2011).

The remaining variables in (6) $(\psi_{(n+1)}, u_{(n+1)}, r_{(n+1)})$ could be replaced by a function of $(\psi_{ez(n+1)}, u_{ez(n+1)}, r_{ez(n+1)})$, where $(\psi_{ez(n+1)}, u_{ez(n+1)}, r_{ez(n+1)})$ represents the values so that (6) has an exact solution and:

$$\psi_{(n+1)} = \psi_{ez(n+1)} - k_\psi\ (\psi_{ez(n)} - \psi_{(n)}) \tag{9}$$

$$u_{(n+1)} = u_{ez(n+1)} - k_u\ (u_{ez(n)} - u_{(n)}) \tag{10}$$

$$r_{(n+1)} = r_{ez(n+1)} - k_r\ (r_{ez(n)} - r_{(n)}) \tag{11}$$

where k_u, k_r *and* k_ψ are controller's parameters and fulfil $0<k_u<1$, $0<k_r<1$ and $0<k_\psi<1$ to the tracking error tends to zero (see Appendix).

Considering equations (7)-(11) the system (6) can be rewritten as:

$$\begin{bmatrix} 0 & 0 \\ 0 & 0 \\ 0 & 0 \\ 0 & 0 \\ \frac{1}{m_{11}} & 0 \\ 0 & \frac{1}{m_{33}} \end{bmatrix} \begin{bmatrix} T_{u(n)} \\ T_{r(n)} \end{bmatrix} =$$

$$= \begin{bmatrix} \left(\frac{x_{ref(n+1)} - k_x\ (x_{ref(n)} - x_{(n)}) - x_{(n)}}{T_0}\right) - \left(u_{(n)}\cos(\psi_{(n)}) - v_{(n)}\sin(\psi_{(n)})\right) \\ \left(\frac{y_{ref(n+1)} - k_y\ (y_{ref(n)} - y_{(n)}) - y_{(n)}}{T_0}\right) - \left(u_{(n)}\sin(\psi_{(n)}) + v_{(n)}\cos(\psi_{(n)})\right) \\ \left(\frac{\psi_{ez(n+1)} - k_\psi\ (\psi_{ez(n)} - \psi_{(n)}) - \psi_{(n)}}{T_0}\right) - r_{(n)} \\ \left(\frac{v_{(n+1)} - v_{(n)}}{T_0}\right) - \left(-\frac{m_{11}}{m_{22}} u_{(n)}\ r_{(n)} - \frac{d_{22}}{m_{22}} v_{(n)}\right) \\ \left(\frac{u_{ez(n+1)} - k_u\ (u_{ez(n)} - u_{(n)}) - u_{(n)}}{T_0}\right) - \left(\frac{m_{22}}{m_{11}} v_{(n)}\ r_{(n)} - \frac{d_{11}}{m_{11}} u_{(n)}\right) \\ \left(\frac{r_{ez(n+1)} - k_r\ (r_{ez(n)} - r_{(n)}) - r_{(n)}}{T_0}\right) - \left(\frac{m_{11} - m_{22}}{m_{33}} v_{(n)}\ u_{(n)} - \frac{d_{33}}{m_{33}} r_{(n)}\right) \end{bmatrix} \tag{12}$$

The first four rows in the system (12) represent the conditions to be fulfilled so that (12) has a solution under the constraints (9) – (11). To solve this problem the first two row of system (12) are written in the form:

$$\underbrace{\begin{bmatrix} \cos(\psi_{(n)}) \\ \sin(\psi_{(n)}) \end{bmatrix}}_{A} \underbrace{u_{(n)}}_{u} = \underbrace{\begin{bmatrix} \left(\frac{x_{ref(n+1)} - k_x\ (x_{ref(n)} - x_{(n)}) - x_{(n)}}{T_0}\right) - v_{(n)}\sin(\psi_{(n)}) \\ \left(\frac{y_{ref(n+1)} - k_y\ (y_{ref(n)} - y_{(n)}) - y_{(n)}}{T_0}\right) - v_{(n)}\cos(\psi_{(n)}) \end{bmatrix}}_{b} \tag{13}$$

Then, $\psi_{ez(n)}$, and $u_{ez(n)}$ are determined such that:

$$\begin{bmatrix} \cos(\psi_{ez(n)}) \\ \sin(\psi_{ez(n)}) \end{bmatrix} u_{ez(n)} = b \tag{14}$$

By a simple calculation is obtained:

$$\tan(\psi_{ez(n)}) = \frac{\sin(\psi_{ez(n)})}{\cos(\psi_{ez(n)})} = \frac{\frac{y_{ref(n+1)} - k_y(y_{ref(n)} - y_{(n)}) - y_{(n)}}{T_0} - v_{(n)}\ \cos(\psi_{(n)})}{\frac{x_{ref(n+1)} - k_x(x_{ref(n)} - x_{(n)}) - x_{(n)}}{T_0} + v_{(n)}\ \sin(\psi_{(n)})} \tag{15}$$

and

$$u_{ez(n)} = \left(\frac{y_{ref(n+1)} - k_y \left(y_{ref(n)} - y_{(n)}\right) - y_{(n)}}{T_0} - v_{(n)} \cos(\psi_{(n)}) \right) \sin(\psi_{ez(n)}) + \ldots$$
$$\ldots + \left(\frac{x_{ref(n+1)} - k_x \left(x_{ref(n)} - x_{(n)}\right) - x_{(n)}}{T_0} + v_{(n)} \sin(\psi_{(n)}) \right) \cos(\psi_{ez(n)}) \tag{16}$$

Next, the yaw velocity is analysed. Considering the third row of (12) and (15), we defined:

$$r_{ez(n)} = \frac{\psi_{ez(n+1)} - k_\psi \left(\psi_{ez(n)} - \psi_{(n)}\right) - \psi_{(n)}}{T_0} \tag{17}$$

where $e_{\psi(n)}=\psi_{ez(n)}-\psi_{(n)}$ is the orientation error. The controller parameter k_ψ fulfil $0<k_\psi<1$ to the tracking error tends to zero (see Appendix). The expressions $u_{ez(n)}$ and $r_{ez(n)}$ represent the desired value of u and r for the tracking error ($e_{(n)}$) tends to zero. Thus, from (12), (17) and (18) the system (19) is defined,

$$\begin{bmatrix} \frac{1}{m_{11}} & 0 \\ 0 & \frac{1}{m_{33}} \end{bmatrix} \begin{bmatrix} T_{u(n)} \\ T_{r(n)} \end{bmatrix} = \ldots$$
$$\ldots = \begin{bmatrix} \frac{u_{ez(n+1)} - k_u \left(u_{ez(n)} - u_{(n)}\right) - u_{(n)}}{T_0} - \frac{m_{22}}{m_{11}} v_{(n)}\, r_{(n)} + \frac{d_{11}}{m_{11}} u_{(n)} \\ \frac{r_{ez(n+1)} - k_r \left(r_{ez(n)} - r_{(n)}\right) - r_{(n)}}{T_0} - \frac{m_{11} - m_{22}}{m_{33}} v_{(n)}\, u_{(n)} + \frac{d_{33}}{m_{33}} r_{(n)} \end{bmatrix} \tag{18}$$

where k_u and k_r are controller's parameters and fulfil that $0<k_u<1$ and $0<k_r<1$ to the tracking error tends to zero (see Appendix). In (19) the values of $T_{u(n)}$ and $T_{r(n)}$ represent the control actions necessary so that the marine vessel reach and follow a pre-established trajectory. Then, resolving the system of linear equations (19) the proposed controller for the Marine Vessel is given by,

$$\begin{bmatrix} T_{u(n)} \\ T_{r(n)} \end{bmatrix} = \begin{bmatrix} m_{11} \left(\frac{u_{ez(n+1)} - k_u \left(u_{ez(n)} - u_{(n)}\right) - u_{(n)}}{T_0} - \frac{m_{22}}{m_{11}} v_{(n)}\, r_{(n)} + \frac{d_{11}}{m_{11}} u_{(n)} \right) \\ m_{33} \left(\frac{r_{ez(n+1)} - k_r \left(r_{d(n)} - r_{(n)}\right) - r_{(n)}}{T_0} - \frac{m_{11} - m_{22}}{m_{33}} v_{(n)}\, u_{(n)} + \frac{d_{33}}{m_{33}} r_{(n)} \right) \end{bmatrix} \tag{19}$$

Theorem 1: If the system behaviour is ruled by (6) and the controller is designed by (15),(16),(17) and (19). Then, $e_{(n)} \rightarrow 0, n \rightarrow \infty$, when trajectory tracking problems are considered.

The proof of Theorem 1 and the convergence to zero of tracking errors can be seen in Appendix.

In the proposed methodology first, the reference speeds are identified so that the error tends to zero and then the control actions are calculated to keep the velocity profile obtained. This controller structure arises naturally when the conditions for the system in (6) are analysed to have exact solution.

3. SIMULATIONS RESULTS

3.1 Simulations Configuration

In this section, we carry out computer simulations to demonstrate the performance of our tracking controller. The control approach is applied on the original time-continuous system. The marine vessel configuration is obtained from recent papers (Bao-li, 2009; Ghommam et al., 2009), it has a length of 1.19 m, and a mass of 17.6 kg and is represented for the following parameters: $m_{11}=19$ *kg*, $m_{22}=35.2$ *kg*, $m_{33}=4.2$ *kg*, $d_{11}=4$ $kg \cdot s^{-1}$, $d_{22}=1$ $kg \cdot s^{-1}$, $d_{33}=10$ $kg \cdot s^{-1}$.

In order to perform realistic simulations, saturation levels in the control signals are imposed, (Lefeber et al., 2003): $T_{umax}=1$ *N*, $T_{umin}= -1$ *N*, $T_{rmax}=1$ $N \cdot m$, $T_{rmin}= -1$ $N \cdot m$. The reference trajectory is a straight-line for the first 20 m generated with constant linear velocity and, then followed by a circumference of 4 m radius with constant speed different from the speed used to generate the straight line. Thus, the performance of the system, when the speed of the reference trajectory changes abruptly, will be analysed. The reference trajectory starts at (2,0)m and the sampling time T_0 used for the simulation is 0.1 sec. The initial condition of the ship simulation is $x(0)=0m$; $y(0)=-1m$; $\psi(0)=0rad$; $u(0)=0m/s$; $v(0)=0m/s$; $r(0)=0rad/s$. The controller's parameters are chosen by empirical tests:

$$\begin{bmatrix} k_x & k_y & k_u & k_r & k_\psi \end{bmatrix} = \begin{bmatrix} 0.93 & 0.93 & 0.4 & 0.4 & 0.16 \end{bmatrix}$$

In Fig. 2 is shown a flowchart to explaining how the controller is applied in the ship control. Figure 3 shows the architecture of the strategy presented herein.

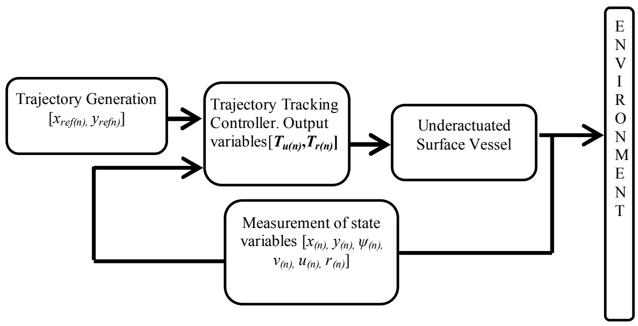

Fig. 2. Architecture of the trajectory tracking controller.

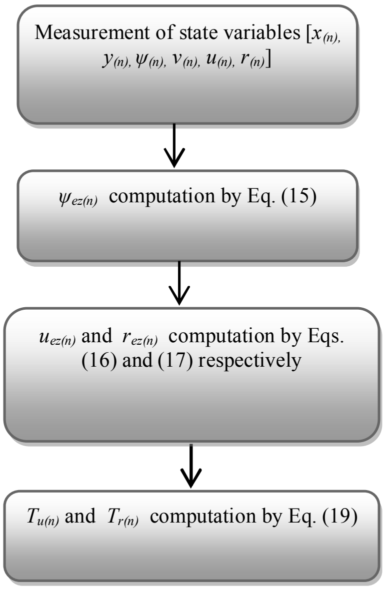

Fig. 3. Flowchart of the strategy proposed.

3.2 Simulation Results without Environmental Disturbances

To verify the theoretical results presented in this paper, a simulation without environmental disturbances was performed. Fig. 4 shows that the ship tends to the reference trajectory and the error tends to zero as shown in Fig. 7. The trajectory in x and y versus time along, with their respective reference values (x_{ref} and y_{ref}) are shown in Fig. 5 and Fig. 6. The control signals are shown in Fig. 8 and Fig. 9.

Figure 4 shows how the ship reaches the reference trajectory quickly and then continues without undesirable oscillations. When there is an abrupt change in reference speed, this produces an increase of the errors of x and y, but later they tend to zero. This convergence can be seen in Fig. 5 and Fig. 6. Figure 7 shows how the tracking error tends to zero. Figures 8 and 9 shows how the control actions have no undesirable oscillations, when there is a change in reference speed of the trajectory. The processing time used to compute the values of the control variables is shown in Fig. 10. This shows how the processing values remain below the sampling time (T_0) used for the simulation. Therefore the performance of the tracking system is satisfactory.

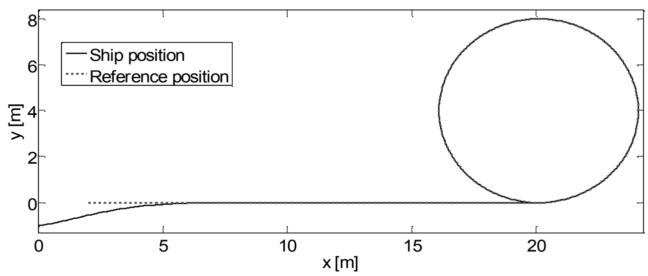

Fig. 4. Tracking Trajectory in the (x,y) plane.

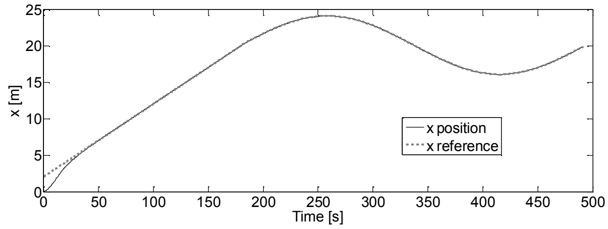

Fig. 5. Tracking position: x vs. time. The graph shows how the state variable follows the reference value.

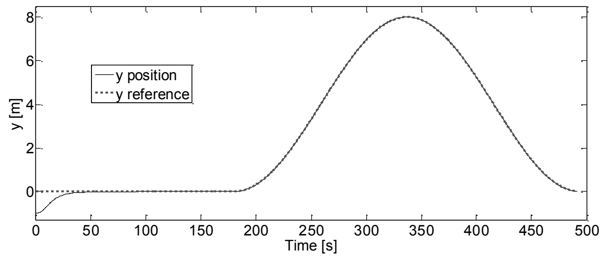

Fig. 6. Tracking position: y vs. time. The graph shows how the state variable follows the reference value.

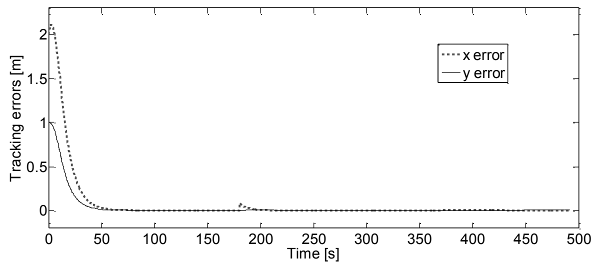

Fig. 7. Tracking errors vs. time.

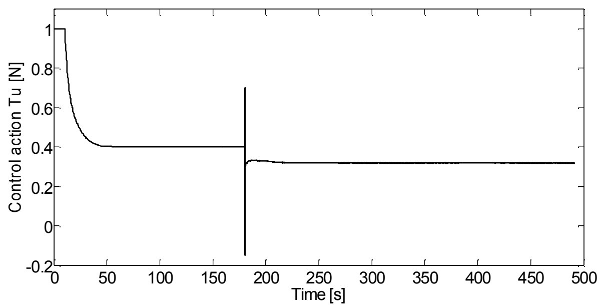

Fig. 8. Control Action T_u vs. time.

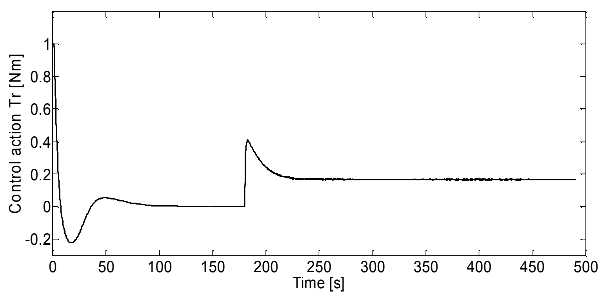

Fig. 9. Control Action T_r vs. time.

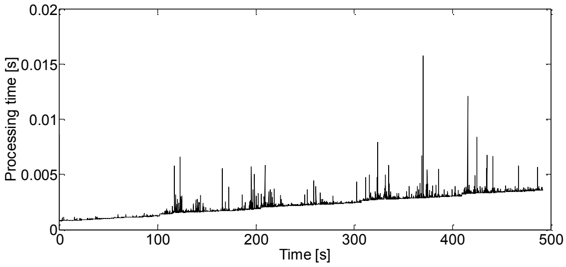

Fig. 10. Processing time vs. time.

3.3 Simulation results with environmental disturbances

To test the robustness of the proposed controller with respect to small environmental disturbances induced by wave, wind and ocean-current (Do et al., 2002a), we simulate the control law (20) with the same design constants selected above. Figs. 11, 12, 13 and 14 plot the simulation results with the environmental disturbances acting on the surge, sway and yaw dynamics as $T_{wu}=0.005m_{11}rand(\cdot)$, $T_{wv}=0.0025m_{22}rand(\cdot)$, $T_{wr}=0.02m_{33}rand(\cdot)$, where $rand(\cdot)$ is the random noise with a magnitude of 1 and zero lower bound. This choice results in non-zero-mean disturbances. The above disturbances are represented as follows:

$$\begin{cases} \dot{u} = \dfrac{m_{22}}{m_{11}} v\, r - \dfrac{d_{11}}{m_{11}} u + \dfrac{1}{m_{11}} T_u + \dfrac{1}{m_{11}} T_{wu} \\ \dot{v} = -\dfrac{m_{11}}{m_{22}} u\, r - \dfrac{d_{22}}{m_{22}} v + \dfrac{1}{m_{22}} T_{wv} \\ \dot{r} = \dfrac{m_{11} - m_{22}}{m_{33}} v\, u - \dfrac{d_{33}}{m_{33}} u + \dfrac{1}{m_{33}} T_r + \dfrac{1}{m_{33}} T_{wr} \end{cases} \tag{20}$$

The disturbance model has been used in recent works (Do et al., 2002a; Do et al., 2004; Ghommam et al., 2009). However, in practice disturbances may be different.

In Fig. 11, it can be seen that the ship tends to the reference trajectory and after reaching the desired value, it keeps on without unwanted oscillations. The trajectory in x and y with their respective reference values (x_{ref} and y_{ref}) are shown in Figs. 12 and 13. These show how the convergences of variables to their reference values are not affected by perturbations. Figure 14 shows how the tracking errors x and y are small despite the perturbations. Control actions result obtained are plotted in Figs. 15 and 16. The processing time necessary to compute the values of the control variables is shown in Fig. 17.

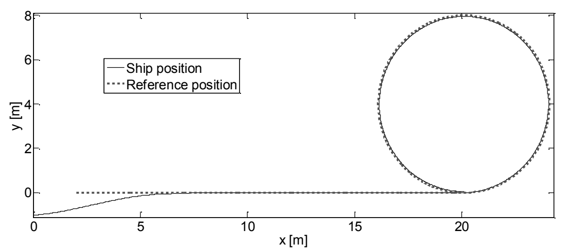

Fig. 11. Tracking Trajectory in the (x,y) plane in presence of environmental disturbances.

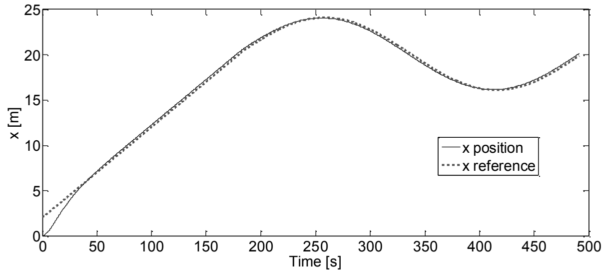

Fig. 12. Tracking position: x vs. time (with environmental disturbances).

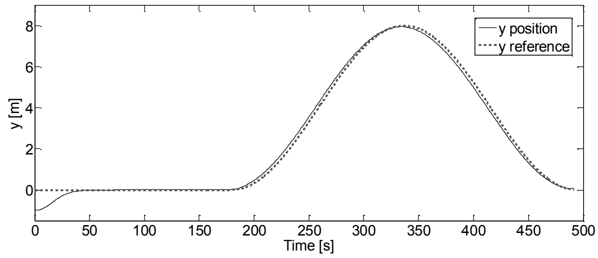

Fig. 13. Tracking position: y vs. time (with environmental disturbances).

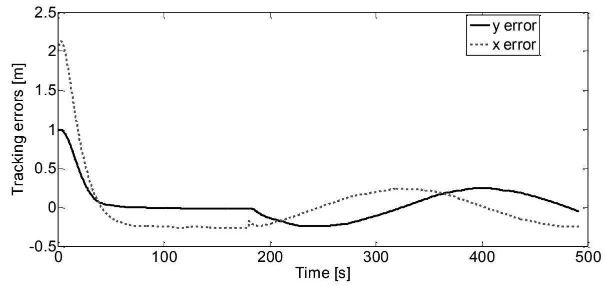

Fig. 14. Tracking errors vs. time in presence of environmental disturbances.

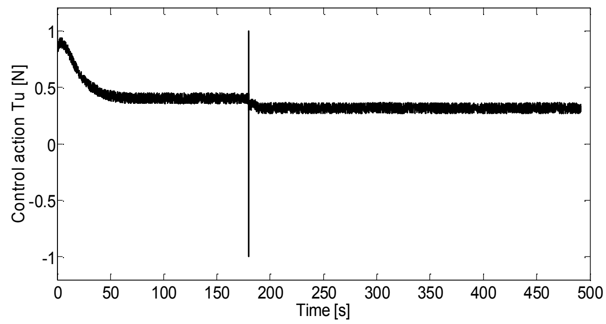

Fig. 15. Control Action T_u vs. time (with environmental disturbances).

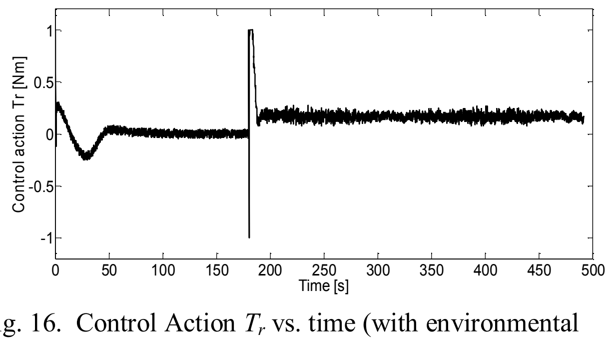

Fig. 16. Control Action T_r vs. time (with environmental disturbances).

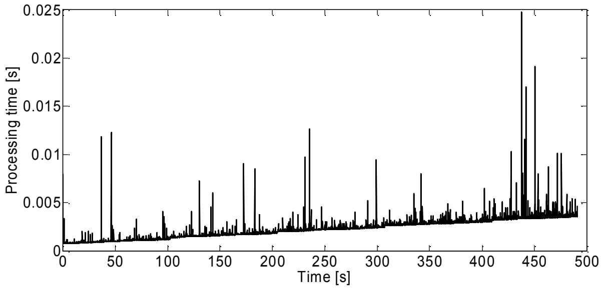

Fig. 17. Processing time vs. time (with environmental disturbances).

The above figures show that the controller proposed in this work presents a certain level of robustness to environmental disturbances. These disturbances were not considered in the design of the controller. However, the empirical tests carried out show the good performance of the control law.

4. CONCLUSIONS

In this paper, the trajectory tracking problem of the underactuated marine surface vessels has been considered. The main contribution of this work is a new methodology to design control algorithms for trajectory tracking of surface vessels based on linear algebra. The methodology is based on the search for conditions under which a system of linear equations has an exact solution. These conditions establish the desired values of orientation, linear speed, angular speed and finally the control actions for that the tracking error goes to zero, as shown in Appendix. One advantage of the methodology applied is that knowing the system model only needs x_{ref}, y_{ref} to calculate the control actions. Compared to (Scaglia et al., 2008; Scaglia et al., 2009; Rosales et al., 2011), this work has included the demonstration of convergence to zero of the tracking errors.

Simulation results show the effectiveness of the proposed controller. Besides, when the system's behaviour is tested to disturbances, it can be seen that its performance is very good compared to the results obtained by (Do et al., 2002a). Compared to (Ghommam et al., 2006; Ghommam et al., 2009), the above control structures can be designed and implemented without great difficulty if it has the speed and position of the ship, because standard algebraic-numerical techniques are used. In comparison with others previous published control laws (Lefeber et al., 2003; Zheng and Jun 2012), the method proposed here, does not need a coordinate transformation. In addition, our controller does not present the disadvantage of (Do et al., 2002b and Jiang, 2002), where it's imposed that the yaw velocity to be non-zero. Furthermore, here it is not necessary to linearize the system as in (Oh and Sun, 2010).

The proposed controller presents the advantages of being easy to design and to implement, the algorithm can be implemented directly on the ship's microcontroller without the need to implement it on an external computer, because the calculations are simple to perform. The developed methodology for the controller design can be applied to other types of systems. The possibility to include in the controller design the saturation of the control signals and observer-controller schemes, as shown in (Wondergem et al., 2011), will be addressed in future contributions.

REFERENCES

Bao-li M. (2009). Global k-exponential asymptotic stabilization of underactuated surface vessels. *Systems & Control Letters*, 58, pp. 194-201.

Do K.D., Jiang Z.P. and Pan J. (2002). Robust global stabilization of underactuated ships on a linear course: state and output feedback. *Proc. American Control Conf.*, 2002, pp. 1687–1692.

Do K.D., Jiang Z.P. and Pan J. (2002). Universal controllers for stabilization and tracking of underactuated ships. *Systems & Control Letters*, 47 (2002).

Do K.D., Jiang Z.P. and Pan J. (2004). Robust adaptive path following of underactuated ships. *Automatica*, 40, pp. 929–944.

Ghommam J., Mnif F. and Derbel N. (2009). Global stabilisation and tracking control of underactuated surface vessels. *IET Control Theory and Applications*, ISSN 1751-8644.

Ghommam J., Mnif F., Benali A., and Derbel N. (2006). Asymptotic Backstepping Stabilization of an Underactuated Surface Vessel. *IEEE Transactions on Control Systems Technology*, vol. 14, no. 6.

Jiang Z.P. (2002). Global tracking control of underactuated ships by Lyapunov's direct method. *Automatica*, 38, (2), pp. 301–309.

Lefeber E., Pettersen K. Y., and Nijmeijer H. (2003). Tracking Control of an Underactuated Ship. *IEEE Transactions on Control Systems Technology*, vol. 11, no. 1.

Oh S. and Sun J. (2010). Path following of underactuated marine surface vessels using line-of-sight based model predictive control. *IEEE Journal Ocean. Eng.*, vol. 37, pp. 289–295.

Rosales A., Scaglia G.J.E., Mut M. and Di Sciascio F. (2011). Formation control and trajectory tracking of mobile robotic systems – a Linear Algebra approach. *Robotica*, v. 29, pp. 335-349.

Rosales A., Scaglia G.J.E., Mut V. and Di Sciascio F., (2009). Trajectory tracking of mobile robots in dynamic environments a linear algebra approach. *Robotica Cambridge University Press* volume 27, pp. 981–997 doi: 10.1017/S0263574709005402, (2009).

Scaglia G.J.E., Quintero L., Mut V. and Di Sciascio F. (2008). Numerical methods based controller design for mobile robots. *Proceedings of the 17th World Congress and the International Federation of Automatic Control (IFAC), Seoul, Korea*, July 6-11, 2008, pp. 4820-4827.

Scaglia G.J.E., Quintero L., Mut V. and Di Sciascio F. (2009). Numerical Methods Based Controller Design for Mobile Robots. *Robotica*, Volume 27, Issue 02, pp. 269-279.

Scaglia G.J.E., Rosales A., Quintero L., Mut V. and Agarwal R. (2010). A Linear-Interpolation-based Controller Design for Trajectory Tracking of Mobile Robots. *Control Engineering Practice,* v. 18, pp. 318–329.

Strang G. (1980). Linear Algebra and Its Applications. *Academic Press, New York*, 1980.
Wondergem M., Lefeber E., Pettersen K. Y., and Nijmeijer H. (2011). Output Feedback Tracking of Ships. *IEEE Transactions on Control Systems Technology*, vol. 19, no. 2.
Zheng Y. and Jun W. (2012). Model Predictive Control for Tracking of Underactuated Vessels Based on Recurrent Neural Networks. *IEEE Journal Ocean. Eng.,* v. 37.

APPENDIX A.

Proof of Theorem 1: if the system's behaviour is ruled by (6), and the controller is designed by (20), when $n \to \infty$ (with $n \in N$) then, $\left\| e_{(n)} \right\| = \sqrt{\left(e_{x(n)}{}^2 + e_{y(n)}{}^2 \right)} \to 0$.

Remark 5: consider the next geometric progression,

$$a_{(1)} = ka_{(0)}$$
$$a_{(2)} = ka_{(1)} = k^2 a_{(0)}$$
$$\vdots$$
$$a_{(n+1)} = ka_{(n)} = k^n a_{(0)}$$

Then, if $0 < k < 1$ and $n \to \infty$ (with $n \in N$), then $a_{(n)} \to 0$.

The proof of convergence to zero of the tracking errors is started with the variable *u*. By replacing the control action $T_{u(n)}$ given by (19) in (6), the following expression is found:

$$\underbrace{u_{ez(n+1)} - u_{(n+1)}}_{e_{u(n+1)}} = k_u \underbrace{\left(u_{ez(n)} - u_{(n)} \right)}_{e_{u(n)}} \tag{A.1}$$

$$e_{u(n+1)} = k_u e_{u(n)} \tag{A.2}$$

Then if $0 < k_u < 1$ and $n \to \infty$ (with $n \in N$), it holds that $e_{u(n)} \to 0$ (see Remark 5).

Using a similar procedure as above, the analysis of variable $e_{r(n)}$ is developed below. Then, considering the control action $T_{r(n)}$ (19) and replacing in (6),

$$\underbrace{r_{ez(n+1)} - r_{(n+1)}}_{e_{r(n+1)}} = k_r \underbrace{\left(r_{ez(n)} - r_{(n)} \right)}_{e_{r(n)}} \tag{A.3}$$

$$e_{r(n+1)} = k_r e_{r(n)} \tag{A.4}$$

Then if $0 < k_r < 1$, it holds that $e_{r(n)} \to 0$ when $n \to \infty$, with $n \in N$ (see Remark 5).

The same analysis applies to variable ψ. From (6) and (A.3),

$$\psi_{(n+1)} = \psi_{(n)} + T_0 \underbrace{\left(r_{ez(n)} - e_{r(n)} \right)}_{r_{(n)}} \tag{A.5}$$

From (2) and (A.5),

$$\psi_{(n+1)} = \psi_{(n)} + T_0 \left(\frac{\psi_{ez(n+1)} - k_\psi \left(\psi_{ez(n)} - \psi_{(n)} \right) - \psi_{(n)}}{T_0} - e_{r(n)} \right) \tag{A.6}$$

Operating,

$$\psi_{ez(n+1)} - \psi_{(n+1)} = k_\psi \left(\psi_{ez(n)} - \psi_{(n)} \right) \psi_{(n)} - T_0 e_{r(n)} \tag{A.7}$$

Then,

$$e_{\psi(n+1)} = k_\psi \; e_{\psi(n)} + T_0 \; e_{r(n)} \tag{A.8}$$

Finally, how $0 < k_\psi < 1$ and $e_{r(n)} \to 0$ when $n \to \infty$, the guidance error $e_{\psi(n)}$ tend to 0 when $n \to \infty$, whit $n \in N$ (see Remark 5).

Now, the convergence analysis of e_x and e_y is developed below.

From the corresponding equation of the system (6),

$$x_{(n+1)} = x_{(n)} + T_0 \left(u_{(n)} \cos(\psi_{(n)}) - v_{(n)} \sin(\psi_{(n)}) \right) \tag{A.9}$$

Considering $e_{u(n)}$ from (A.1) and replacing in (A.9),

$$x_{(n+1)} = x_{(n)} + T_0 \left(u_{ez(n)} \cos(\psi_{(n)}) - v_{(n)} \sin(\psi_{(n)}) \right) - T_0 \; e_{u(n)} \cos(\psi_{(n)}) \tag{A.10}$$

The Taylor approximation of $\cos(\psi_{(n)})$ in the desired value $\psi_{ez(n)}$ is:

$$\cos(\psi_{(n)}) = \cos(\psi_{ez(n)}) - \sin\left(\psi_{ez(n)} + \zeta \left(\psi_{(n)} - \psi_{ez(n)} \right) \right) \left(\psi_{(n)} - \psi_{ez(n)} \right); 0 < \zeta < 1 \tag{A.11}$$

Defining $e_{\psi(n)} = \psi_{ez(n)} - \psi_{(n)}$ as the error in ψ :

$$\cos(\psi_{(n)}) = \cos(\psi_{ez(n)}) + \sin\left(\psi_{ez(n)} - \zeta e_{\psi(n)} \right) e_{\psi(n)}; 0 < \zeta < 1 \tag{A.12}$$

By replacing (A.12) in (A.10):

$$x_{(n+1)} = x_{(n)} + T_0 \left(u_{ez(n)} \cos(\psi_{ez(n)}) - v_{(n)} \sin(\psi_{(n)}) \right) - T_0 \left(e_{u(n)} \cos(\psi_{(n)}) - u_{ez(n)} e_{\psi(n)} \sin\left(\psi_{ez(n)} - \zeta e_{\psi(n)} \right) \right) \tag{A.13}$$

By defining:

$$f_{(n)} = -T_0 \left(e_{u(n)} \cos(\psi_{(n)}) - u_{ez(n)} e_{\psi(n)} \sin\left(\psi_{ez(n)} - \zeta e_{\psi(n)} \right) \right) \tag{A.14}$$

Then, considering (A.14) and $u_{ez(n)}$ from (16), and replacing in (A.13):

$$x_{(n+1)} = x_{(n)} + T_0\left(\left(\left(\left(\frac{y_{ref(n+1)} - k_y\ (y_{ref(n)} - y_{(n)}) - y_{(n)}}{T_0} - v_{(n)}\cos(\psi_{(n)})\right)\right.\right.\right.$$
$$\cdot\sin(\psi_{ez(n)}) + \left(\frac{x_{ref(n+1)} - k_x\ (x_{ref(n)} - x_{(n)}) - x_{(n)}}{T_0} + v_{(n)}\sin(\psi_{(n)})\right)$$
$$\left.\left.\left.\cdot\cos(\psi_{ez(n)})\right)\cos(\psi_{ez(n)}) - v_{(n)}\sin(\psi_{(n)})\right)\right) + f_{(n)} \tag{A.15}$$

From (15),

$$y_{ref(n+1)} - k_y(y_{ref(n)} - y_{(n)}) - y_{(n)} - v_{(n)}\ \cos(\psi_{(n)})$$
$$= \left(x_{ref(n+1)} - k_x(x_{ref(n)} - x_{(n)}) - x_{(n)} + v_{(n)}\ \sin(\psi_{(n)})\right)\frac{\sin(\psi_{ez(n)})}{\cos(\psi_{ez(n)})} \tag{A.16}$$

Then, replacing (A.16) in (A.15):

$$x_{(n+1)} = x_{(n)} + T_0\left(\left(x_{ref(n+1)} - k_x(x_{ref(n)} - x_{(n)}) - x_{(n)} + v_{(n)}\ \sin(\psi_{(n)})\right)\right.$$
$$\cdot\sin^2(\psi_{ez(n)}) + \left(x_{ref(n+1)} - k_x(x_{ref(n)} - x_{(n)}) - x_{(n)} + v_{(n)}\ \sin(\psi_{(n)})\right)$$
$$\left.\cdot\cos^2(\psi_{ez(n)}) - v_{(n)}\sin(\psi_{(n)})\right) + f_{(n)} \tag{A.17}$$

Then:

$$x_{(n+1)} = x_{(n)} + T_0\left(x_{ref(n+1)} - k_x(x_{ref(n)} - x_{(n)}) - x_{(n)}\right) + f_{(n)} \tag{A.18}$$

Operating:

$$\underbrace{x_{ref(n+1)} - x_{(n+1)}}_{e_{x(n+1)}} = k_x(\underbrace{x_{ref(n)} - x_{(n)}}_{e_{x(n)}}) + f_{(n)} \tag{A.19}$$

From (A.19),

$$e_{x(n+1)} - k_x\ e_{x(n)} + f_{(n)} = 0 \tag{A.20}$$

Finally discuss $e_{y(n)}$ of the same way that previous case. From the corresponding equation of the system (6),

$$y_{(n+1)} = y_{(n)} + T_0\ \left(u_{(n)}\ \sin(\psi_{(n)}) - \mathrm{v}_{(n)}\ \cos(\psi_{(n)})\right) \tag{A.21}$$

Considering $e_{u(n)}$ from (A.1) and replacing in (A.21),

$$y_{(n+1)} = y_{(n)} + T_0\ \left(u_{ez(n)}\sin(\psi_{(n)}) + \mathrm{v}_{(n)}\ \cos(\psi_{(n)})\right) - T_0 e_{u(n)}\sin(\psi_{(n)}) \tag{A.22}$$

The Taylor approximation of $\sin(\psi_{(n)})$ in the desired value $\psi_{ez(n)}$ is:

$$\sin(\psi_{(n)}) = \sin(\psi_{ez(n)})$$
$$+\cos\left(\psi_{ez(n)} + \theta\left(\psi_{(n)} - \psi_{ez(n)}\right)\right)\left(\psi_{(n)} - \psi_{ez(n)}\right); 0 < \theta < 1 \tag{A.23}$$

Considering $e_{\psi(n)}$:

$$\sin(\psi_{(n)}) = \sin(\psi_{ez(n)}) + \cos\left(\psi_{ez(n)} + \theta e_{\psi(n)}\right)e_{\psi(n)}; 0 < \theta < 1 \tag{A.24}$$

By replacing (A.24) in (A.22):

$$y_{(n+1)} = y_{(n)} + T_0\ \left(u_{ez(n)}\sin(\psi_{ez(n)}) + \mathrm{v}_{(n)}\ \cos(\psi_{(n)})\right)$$
$$-T_0\left(e_{u(n)}\sin(\psi_{(n)})\ \text{-}u_{ez(n)}e_{\psi(n)}\cos\left(\psi_{ez(n)} - \theta e_{\psi(n)}\right)\right) \tag{A.25}$$

By defining:

$$g_{(n)} = -T_0\ \left(e_{u(n)}\sin(\psi_{(n)}) - u_{ez(n)}e_{\psi(n)}\cos\left(\psi_{ez(n)} - \theta e_{\psi(n)}\right)\right) \tag{A.26}$$

Then, considering (A.26) and $u_{ez(n)}$ from (16), and replacing in (A.25):

$$y_{(n+1)} = y_{(n)} + T_0\left(\left(\left(\left(\frac{y_{ref(n+1)} - k_y\ (y_{ref(n)} - y_{(n)}) - y_{(n)}}{T_0} - v_{(n)}\cos(\psi_{(n)})\right)\right.\right.\right.$$
$$\cdot\sin(\psi_{ez(n)}) + \left(\frac{x_{ref(n+1)} - k_x\ (x_{ref(n)} - x_{(n)}) - x_{(n)}}{T_0} + v_{(n)}\sin(\psi_{(n)})\right)\cos(\psi_{ez(n)})\Bigg)$$
$$\left.\left.\cdot\sin(\psi_{ez(n)}) + v_{(n)}\sin(\psi_{(n)})\right)\right) + g_{(n)} \tag{A.27}$$

Considering equation (15),

$$x_{ref(n+1)} - k_x(x_{ref(n)} - x_{(n)}) - x_{(n)} + v_{(n)}\ \sin(\psi_{(n)})$$
$$= \left(y_{ref(n+1)} - k_y(y_{ref(n)} - y_{(n)}) - y_{(n)} - v_{(n)}\ \cos(\psi_{(n)})\right)\frac{\cos(\psi_{ez(n)})}{\sin(\psi_{ez(n)})} \tag{A.28}$$

Then, replacing (A.28) in (A.27),

$$y_{(n+1)} = y_{(n)} + T_0\left(\left(y_{ref(n+1)} - k_y(y_{ref(n)} - y_{(n)}) - y_{(n)} - v_{(n)}\ \cos(\psi_{(n)})\right)\right.$$
$$\cdot\cos^2(\psi_{ez(n)}) + \left(y_{ref(n+1)} - k_y(y_{ref(n)} - y_{(n)}) - y_{(n)} - v_{(n)}\ \cos(\psi_{(n)})\right)$$
$$\left.\cdot\sin^2(\psi_{ez(n)}) + v_{(n)}\sin(\psi_{(n)})\right) + g_{(n)} \tag{A.29}$$

Operating,

$$y_{(n+1)} = y_{(n)} + T_0\left(y_{ref(n+1)} - k_y(y_{ref(n)} - y_{(n)}) - y_{(n)}\right) + g_{(n)} \quad (A.30)$$

From (A.30)

$$\underbrace{y_{ref(n+1)} - y_{(n+1)}}_{e_{y(n+1)}} = k_y(\underbrace{y_{ref(n)} - y_{(n)}}_{e_{y(n)}}) + g_{(n)} \quad (A.31)$$

Finally, we get,

$$e_{y(n+1)} - k_y\, e_{y(n)} + g_{(n)} = 0 \quad (A.32)$$

Considering (A.14), (A.20), (A.26) and (A.32), we get:

$$\begin{bmatrix} e_{x(n+1)} \\ e_{y(n+1)} \end{bmatrix} = \underbrace{\begin{bmatrix} k_x & 0 \\ 0 & k_y \end{bmatrix}\begin{bmatrix} e_{x(n)} \\ e_{y(n)} \end{bmatrix}}_{\textit{Linear}\text{ System}} + \ldots$$

$$\ldots + T_0 \underbrace{\begin{bmatrix} -u_{ez(n)}\sin\left(\psi_{ez(n)} - \zeta e_{\psi(n)}\right) & \cos(\psi_{(n)}) \\ -u_{ez(n)}\cos\left(\psi_{ez(n)} - \theta e_{\psi(n)}\right) & \sin\left(\psi_{(n)}\right) \end{bmatrix}\begin{bmatrix} e_{\psi(n)} \\ e_{u(n)} \end{bmatrix}}_{\text{Nonlinearity}} \quad (A.33)$$

The equation (A.33) represents a linear system and a nonlinearity, if $0<k_x<1$ and $0<k_y<1$, then (A.33) tends to zero because $e_{\psi(n)}$ and $e_{u(n)} \to 0$ when $n \to 0$, whit $n \in N$ (see Remark 5). Finally, it is thus demonstrated that $e_{x(n)}$ and $e_{y(n)} \to 0$ when $n \to 0$ (whit $n \in N$), and the tracking error tends to 0.